Chapter 4: Down-regulation of the acetyl-CoA metabolic network in adipose tissue of obese diabetic individuals and recovery after weight loss

Harish Dharuri
Peter A.C. ’t Hoen
Jan B. van Klinken
Peter Henneman
Jeroen F.J. Laros
Mirjam A Lips
Fatiha el Bouazzaoui
Gert-Jan van Ommen
Ignace Janssen
Bert van Ramshorst
Bert A. van Wagensveld
Hanno Pijl
Ko Willems van Dijk
Vanessa van Harmelen

Diabetologia. 2014;57(11):2384-92

ABSTRACT

Aims/Hypothesis

Not all obese individuals develop type-2 diabetes. Why some obese individuals remain normal glucose tolerant (NGT) is not well understood. We hypothesize that the biochemical mechanisms that underlie the function of adipose tissue can help explain the difference between obese individuals with NGT and those with type 2 diabetes.

Methods

RNA-sequencing was used to analyse the transcriptome of samples extracted from visceral adipose tissue (VAT) and subcutaneous adipose tissue (SAT) of obese women with NGT or type 2 diabetes who were undergoing bariatric surgery. The gene expression data was analysed by bioinformatic visualization and statistical analyses techniques.

Results

A network-based approach to distinguish obese individuals with NGT from obese individuals with type 2 diabetes identified acetyl-CoA metabolic network down-regulation as an important feature in the pathophysiology of obese individuals with type 2 diabetes. In general, genes within two reaction steps of acetyl-CoA were found to be down-regulated in the VAT and SAT of individuals with type 2 diabetes. Upon weight loss and amelioration of metabolic abnormalities three months following bariatric surgery, the expression level of these genes recovered to levels seen in NGT individuals. We report four novel genes associated with type-2 diabetes and recovery upon weight loss: acetyl-CoA acetyltransferase 1 (*ACAT1*), acetyl-CoA carboxylase alpha (*ACACA*), aldehyde dehydrogenase 6 family, member A1 (*ALDH6A1*) and methylenetetrahydrofolate dehydrogenase (*MTHFD1*).

Conclusion/Interpretation

Down-regulation of the acetyl-CoA network in VAT and SAT is an important feature in the pathophysiology of type 2 diabetes in obese individuals. ACAT1, ACACA, ALDH6A1 and MTHFD1 represent novel biomarkers in adipose tissue associated with type 2 diabetes in obese individuals.

INTRODUCTION

Obesity is associated with increased risk of premature death and has reached epidemic proportions in modern societies [1]. Obesity results in decreased life expectancy due to associated metabolic and cardiovascular disorders, as

well as several types of cancer [2, 3]. A majority of obese individuals develop insulin resistance and type-2 diabetes. However, approximately 10-25% of these individuals seem to remain insulin sensitive and metabolically "healthy" [4]. Studies have shown that the expanded adipose tissue serves as an important pathogenic site in the development of type 2 diabetes [5]. Furthermore, the prevalence of metabolically "healthy" obese has been attributed to a normal adipose tissue function [5]. A criterion for distinguishing the obese subtypes is of crucial importance to develop appropriate intervention and prevention strategies for these individuals [6]. Most studies have focussed on developing risk scores based on blood pressure, lipid levels, glucose homeostasis, and inflammatory parameters to distinguish the metabolically "healthy" from the metabolically abnormal [7, 8]. However, the biological mechanisms underlying the phenotypic differences observed among obese individuals are not fully understood. In view of the central role of adipose tissue in the manifestation of obesity pathology, we investigated gene expression and biochemical pathway profiles in visceral adipose tissue (VAT) and subcutaneous adipose tissue (SAT) in a human cohort comprised of very obese individuals (BMI>40 kg/m^2) who had normal glucose tolerance (NGT) or who had type-2 diabetes.

Whole genome expression profiling of both SAT and VAT presents an opportunity to study the development of disease in the adipose tissue depots and to delineate biological processes explaining the dysregulation of metabolism in these tissues. Earlier studies used microarray analyses to compare gene expression profiles in the SAT and VAT of obese individuals and found co-regulation of immune and metabolic genes with insulin resistance and metabolic syndrome [9-11]. We have employed next-generation RNA sequencing technology as it offers extensive coverage, precise quantitation of transcripts, and a large dynamic range [12-14].

The current study applied bioinformatic visualization and statistical analyses techniques to the gene expression data and showed dysregulated acetyl-CoA metabolism as a distinguishing feature of obese individuals with type 2 diabetes. Multiple genes in the immediate vicinity of the acetyl-CoA reaction network were down-regulated in diabetic obese individuals. To ascertain if the down-regulation of these genes was correlated to health status, we studied expression levels of these genes before and three months after bariatric surgery associated with significant weight loss and improvement of morbidity.

Table 1 Characteristics of participants with NGT and type 2 diabetes at baseline and 3 months post-bariatric surgery

Characteristic	NGT		T2DM		*p* value			
	Baseline	3 months post-surgery	Baseline	3 months post-surgery	T2DM vs NGT (baseline)	T2DM vs NGT (3 months)	NGT 3 months vs baseline	T2DM 3 months vs baseline
n	17	17	15	15				
Age (years)	49±6	49±6	53±5	53±5	NS	NS	NS	NS
BMI (kg/m^2)	42.9±3.2	36.9±3.3	43.4±4.4	35.9±4.0	NS	NS	1.38×10^{-15}	8.21×10^{-16}
Weight (kg)	122.2±3.1	105.0±2.8	118.9±4.5	98.9±3.7	NS	NS	1.23×10^{-14}	2.11×10^{-14}
HOMA-IR	2.79±2.05	1.72±1.62	4.25±3.26	1.68±0.91	0.06	NS	0.09	0.001
Fasting glucose (mmol/l)	5.08±0.54	5.08±0.76	9.28±2.61	5.87±1.21	2.03×10^{-10}	NS	NS	6.9×10^{-8}
Fasting insulin (pmol/l)	72.5±49.9	42.9±34.9	59.4±40.0	38.9±19.7	NS	NS	0.006	0.09
HbA_{1c}								
mmol/mol	37.6±2.3	34.1±0.9	55.0±4.3	40.2±1.8	8.2×10^{-6}	0.10	NS	0.0002
%	5.6	5.3	7.2	5.8	8.2×10^{-6}	0.10	NS	0.0002
Triacylglycerol (mmol/l)	1.49±0.17	1.30±0.13	2.02±0.19	1.32±0.14	0.03	NS	0.03	1.13×10^{-7}
NEFA (mmol/l)	0.99±0.07	1.16±0.08	1.18±0.11	1.14±0.09	NS	NS	0.06	NS
Total cholesterol (mmol/l)	4.84±0.25	4.20±0.18	4.34±0.22	3.49±0.20	NS	0.03	0.002	0.0006
HDL-cholesterol (mmol/l)	1.14±0.07	1.05±0.05	1.10±0.09	1.05±0.07	NS	NS	0.050	NS
LDL-cholesterol (mmol/l)	3.03±0.21	2.42±0.20	2.33±0.17	1.84±0.19	0.02	0.050	0.005	0.053
CRP (mg/l)	7.74±1.90	6.16±2.26	8.30±1.95	4.13±1.00	NS	NS	NS	0.004

Data are means±SD

Statistical differences between NGT and T2DM and pre- and post-intervention groups were determined with a mixed-effects model, where subject- specific deviances were modelled with random intercepts

CRP, C-reactive protein; T2DM, type 2 diabetes

RESEARCH DESIGN AND METHODS

Participants

The study group consisted of 17 obese women with NGT (with normal fasting glucose levels) and 15 obese women with type 2 diabetes (classified according to WHO standards). The groups were matched for age, weight and BMI (Table 1). All the women had been morbidly obese (BMI>40 kg/m2) for at least five years. Participants who reported the use of weight loss medications within 90 days prior to enrolment in the study were excluded. Body weight of all participants had been stable for at least 3 months prior to inclusion. The participants were investigated in the morning after an overnight fast. A venous blood sample was taken for the determination of plasma glucose (by the routine chemistry laboratory at the hospital) and insulin (by IRMA; Medgenix, Fleurus, Belgium). Thereafter, SAT was obtained from the parumbilical region by needle aspiration under local anesthesia using lidocaine. Around four weeks after the first examination all individuals underwent bariatric surgery (gastric bypass/banding). Within 1h after opening the abdominal wall adipose tissue specimens were taken from the epigastric region of the abdominal wall (SAT) and from the major omentum (VAT). One piece of these adipose tissues was immediately put in RNA-later (Ambion®, Life Technologies, Bleiswijk, The Netherlands) and subsequently stored at -80°C. Another piece of adipose tissue was used for the isolation of adipocytes using collagenase treatment, as described [15]. Three months after the operation, the participants were investigated again after an overnight fast. Plasma glucose and insulin was determined and another SAT needle biopsy was taken. The participants were not calorie restricted in the period prior to the bariatric surgery.The study was approved by the Ethics Committee of Leiden University. All participants gave informed consent to participate in the study.

Medication

For obvious reasons we could not restrict to obese participants not using any type of medication. All participants were allowed to use cholesterol lowering statins and antihypertensive medication. The use of drugs such as statins and antihypertensive drugs was slightly higher in the diabetic participants. At baseline, statins were used by 60% of patients with type 2 diabetes and 18% of patients with NGT. Of the diabetic patients 75% used anti-hypertensives against 40% in individuals with NGT. A substantial proportion of patients with

type 2 diabetes received treatment with metformin (n=9; 60%) or sulfonylurea derivatives (n=4; 25%).

Table 2 Top 25 genes up- or downregulated in VAT of diabetic individuals

Gene	Coefficient NGT vs T2DM	p- value NGT vs T2DM	Adjusted p-value NGT vs T2DM
ALDH6A1	-0.670	1.49E-06	0.005502
C14orf45	-0.462	1.59E-06	0.005502
ECHS1	-0.521	1.48E-06	0.005502
IRS1	-0.601	3.41E-07	0.005502
STBD1	-0.615	6.74E-07	0.005502
IARS2	-0.311	2.73E-06	0.006958
NAT8L	-0.745	2.81E-06	0.006958
AIFM2	-0.452	3.24E-06	0.007013
ATPAF1	-0.349	3.71E-06	0.007141
ACAD9	-0.311	8.28E-06	0.010501
GPI	-0.285	8.25E-06	0.010501
HADH	-0.575	8.49E-06	0.010501
HSPD1	-0.299	7.74E-06	0.010501
MTHFD1	-0.423	6.16E-06	0.010501
ACACA	-0.560	9.14E-06	0.010554
MAP3K15	-0.433	1.19E-05	0.012882
HK2	-0.712	1.32E-05	0.01298
PARVG	0.654	1.5E-05	0.01298
PDHA1	-0.375	1.48E-05	0.01298
PRKAR2B	-0.716	1.39E-05	0.01298
ACAT1	-0.406	1.81E-05	0.012994
ATP9A	-0.400	2.1E-05	0.012994
CEBPA	-0.566	1.97E-05	0.012994
DARS2	-0.379	1.64E-05	0.012994
NXPH4	-1.002	1.89E-05	0.012994

Coefficient NGT vs T2DM: log fold change of NGT vs T2DM; a negative value reflects downregulation whereas a positive value reflects upregulation of the gene in type 2 diabetic individuals

For the complete list of up- or downregulated genes in VAT of type 2 diabetic individuals see ESM Table 2

The adjusted *p* value NGT vs T2DM is the *p* value after Benjamini–Hochberg FDR correction

Table 3 Top 25 genes up- or downregulated in SAT of diabetic individuals

Gene	Coefficient NGT vs T2DM	p- value NGT vs T2DM	Adjusted p-value NGT vs T2DM
DHTKD1	-0.39953	3.38E-06	0.027658
DPEP2	0.941324	3.63E-06	0.027658
S100A11	0.389024	4.79E-06	0.027658
IRS1	-0.64306	7.26E-06	0.027696
BIVM	-0.32809	8E-06	0.027696
CRABP2	0.889426	1.15E-05	0.033234
PXMP2	-0.46718	1.65E-05	0.03571
LSP1	0.826079	1.53E-05	0.03571
RNF14	-0.29276	2.01E-05	0.038745
FXYD5	0.508216	3E-05	0.041435
TYROBP	0.789776	2.74E-05	0.041435
CYBA	0.573909	2.8E-05	0.041435
THNSL1	-0.48462	3.11E-05	0.041435
ALDH6A1	-0.59541	5.12E-05	0.042281
C14orf45	-0.39723	0.000107	0.042281
HADH	-0.45138	0.000145	0.042281
MTHFD1	-0.3727	7.95E-05	0.042281
MAP3K15	-0.39465	9.36E-05	0.042281
SLC2A4	-0.73171	0.000105	0.042281
ME1	-0.45845	9.99E-05	0.042281
LDHD	-0.53027	9.59E-05	0.042281
FAN1	-0.26323	5.17E-05	0.042281
TMEM218	-0.39528	0.000128	0.042281
EEPD1	-0.45794	0.000156	0.042281
IL2RG	0.835802	0.000114	0.042281

Coefficient NGT vs T2DM: log fold change of NGT vs T2DM; a negative value reflects downregulation whereas a positive value reflects upregulation of the gene in type 2 diabetic individuals

The adjusted *p* value NGT vs T2DM is the *p* value after Benjamini– Hochberg FDR correction

Isolation of RNA

Total RNA was isolated using the Nucleospin RNA kit (Macherey-Nagel, Düren, Germany) according to the instructions of the manufacturer. The quality of each mRNA sample was examined using the Agilent 2100 Bioanalyzer (Santa Clara, CA). All RNA samples had a RIN value >7.

RNA Deep Sequencing

RNA (fifty µg) of the adipose tissue samples obtained during bariatric surgery were used for RNA deep sequencing which was performed at the Beijing Genomics Institute (BGI) using RNA-Seq (Transcriptome) sequencing on the HiSeq2000 with 90 nucleotide long Paired End reads, resulting in a minimum of 3Gb clean data per sample. The reads were aligned to the Human reference genome build 19 (hg19) to obtain a histogram of coverage per exon and the associated count data (**ESM Methods 1**). Differential expression analysis was done on exon, gene and transcript levels as described in **ESM Methods 1**.

Bioinformatic analysis

The bioinformatic analysis was performed as described in **ESM Methods 2.**

Quantitative Real Time PCR for comparison of pre and post-surgery gene expression data for select members of acetyl-CoA gene set

The RNA of the needle biopsies obtained pre and post bariatric surgery as well as the RNA obtained from the adipocytes during bariatric surgery were used for quantitative real-time PCR (**See ESM Methods 3**).

RESULTS

Characteristics of participants at baseline and three months post-bariatric surgery

Characteristics of the participants are shown in **Table 1**. At baseline fasting glucose, HbA1c and triglyceride levels were significantly higher in individuals with type 2 diabetes than in those with NGT. Three months post-surgery, individuals with NGT and type 2 diabetes showed the same weight-reduction. Fasting glucose, HbA1c and triglyceride levels were significantly reduced in the diabetic individuals and similar to levels in the individuals with NGT.

Gene expression analysis

We utilized RNA-sequencing to analyse the transcriptome of samples extracted from VAT and SAT of 32 (15 with type 2 diabetes, 17 with NGT)

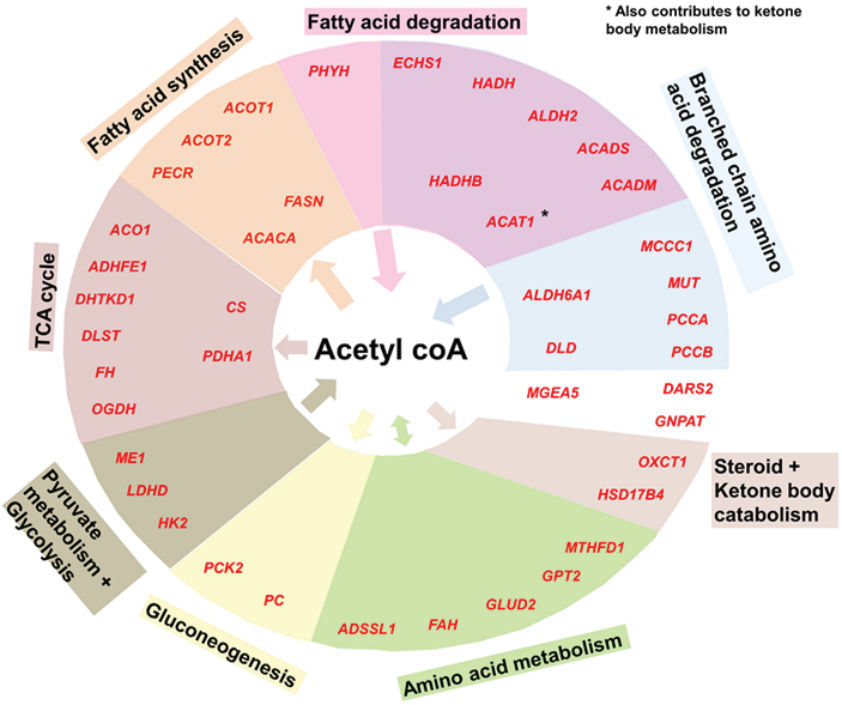

Figure 1 Downregulation of the acetyl-CoA gene network in type 2 diabetes. Forty-two genes that are among the top differentially expressed genes in VAT are also members of the acetyl-CoA gene set. The genes within the inner circle act directly on acetyl-CoA while the genes in the outer circle participate one reaction step away from acetyl-CoA. All the genes were downregulated in VAT. *Also contributes to ketone body metabolism. TCA, tricarboxylic acid cycle

obese female individuals undergoing bariatric surgery (Table 1). We first determined whether the overall gene expression profiles differed between obese women with type 2 diabetes and those with NGT and applied the global test [16] on all expressed genes. The global test on VAT and SAT yielded a p-value of 3.7E-03 and 9.4E-04 respectively indicating a significant association of gene expression with health status.

Gene-level analysis with the limma package in R identified 168 genes differentially expressed in VAT ($p<0.05$, after Benjamin-Hochberg FDR correction) between obese individuals with NGT and those with type 2

diabetes (Table 2 and ESM Table 2). Applying the same method on SAT yielded 121 genes that were significantly differentially expressed between obese individuals with NGT and those with type 2 diabetes (Table 3). There was an overlap of 24 of the differentially expressed genes between the two tissues.

Bioinformatic analysis to identify sub-networks in gene expression data

We further investigated biological mechanisms underlying the differential health status among the participants. Statistically significant differentially expressed genes ($p<0.05$ after FDR correction) in VAT and SAT were used as an input to a pathway-based over-representation analysis tool made available by ConsensusPathDB (http://cpdb.molgen.mpg.de/, accessed 14 January 2013). This analysis of genes from VAT identified pathways relevant to carbon, amino acid and fatty acid metabolism (**ESM Table 3**). A similar analysis strategy for SAT identified pathways relevant to several bacterial infections, regulation of actin cytoskeleton and Fc-Gamma R-mediated phagocytosis (ESM Table 4). The overlap between significant ($q\text{-value}<0.05$) pathways identified for the two tissues is limited to insulin-signalling, branched-chain amino acid degradation and pyruvate metabolism. Furthermore, to determine if significantly differentially expressed genes in each of the two tissues operate in close proximity in network space, we utilized "Network neighbourhood-based entity sets" (NEST) a software tool made available by ConsensusPathDB. ESM Table 5 shows the result for an input of top differentially expressed genes in VAT (168 genes, $p<0.05$ after multiple test correction). This analysis indicated that the differentially expressed genes in VAT operate in a network neighbourhood at the intersection of carbohydrate, amino acid and fatty acid metabolism. Importantly, a majority of the genes mapped onto these pathways were present in close proximity in network space to acetyl-CoA metabolism (Figure 1). A similar approach using NEST with the significant hits from SAT did not yield any statistically significant sets.

The acetyl-CoA metabolic network is down-regulated in diabetic obese individuals

The enriched network neighbourhood-based sets described above hinted at the possibility of acetyl-CoA metabolic network being a common feature of the statistically significant differentially expressed genes in VAT. To evaluate if genes within two reaction steps of acetyl-CoA metabolism were significantly represented among the top hits in VAT, a gene-set was generated using the Taverna workflow management system and the KEGG

pathway database (ESM Methods 4). This approach involved finding all the genes that participate within a radius of 2 steps in the reaction space surrounding acetyl-CoA. This algorithm was implemented in Taverna and the pathway information present in the KEGG database was used to generate the gene set. The total number of genes in the acetyl-CoA set is 419.

We then performed statistical tests to determine if members of the acetyl-CoA gene set were significantly represented among top hits in VAT. The number of genes among the 168 top hits in VAT that are also members of the acetyl-CoA gene set is 42 (ESM Table 2), ten times more than expected by chance (p=1E-63, permutation test), indicating that the presence of the members of acetyl-CoA gene set among the top hits due to chance alone is negligible. All these 42 genes were down regulated in VAT of obese individuals with type 2 diabetes (ESM Table 2). Additionally, the global test to evaluate the acetyl-CoA gene set as a predictor of health status in VAT and SAT yielded a p-value of 2.4E-02 and 8.4E-03 respectively. The network-neighbourhood test did not yield a significant set for SAT, yet the acetyl-CoA gene set is more significant in SAT than in VAT because most of the genes in the acetyl-CoA gene set are borderline significant in SAT. These genes fail to make the cut-off necessary to be included for network neighbourhood tests. However, the global test takes into account the p-value of all the entities in the gene set, and since most genes have modest p-values in SAT, the overall p-value generated for the acetyl-CoA gene set in that tissue type is lower than we would expect by examining the network neighbourhood of the most significant genes. In conclusion, genes in the acetyl-coA reaction network displayed a general down-regulation in both VAT and SAT of individuals with type 2 diabetes.

Analysis at the transcript or exon level

We investigated possible differential splicing events, comparing obese individuals with NGT and type 2 diabetes, for the 42 genes in the acetyl-CoA gene set. To do so, we analysed differences at the 1) transcript level, 2) expression level of individual exons. Of the 42 genes, there were 16 genes with multiple annotated transcripts. All of the transcript variants were significantly down-regulated in the individuals with type 2 diabetes as compared with the individuals with NGT (data not shown).

At the exon level, we did not identify any exon that deviated significantly from the overall gene expression pattern and did not obtain any evidence for alternative splicing between individuals with NGT and those with type 2 diabetes (data not shown).

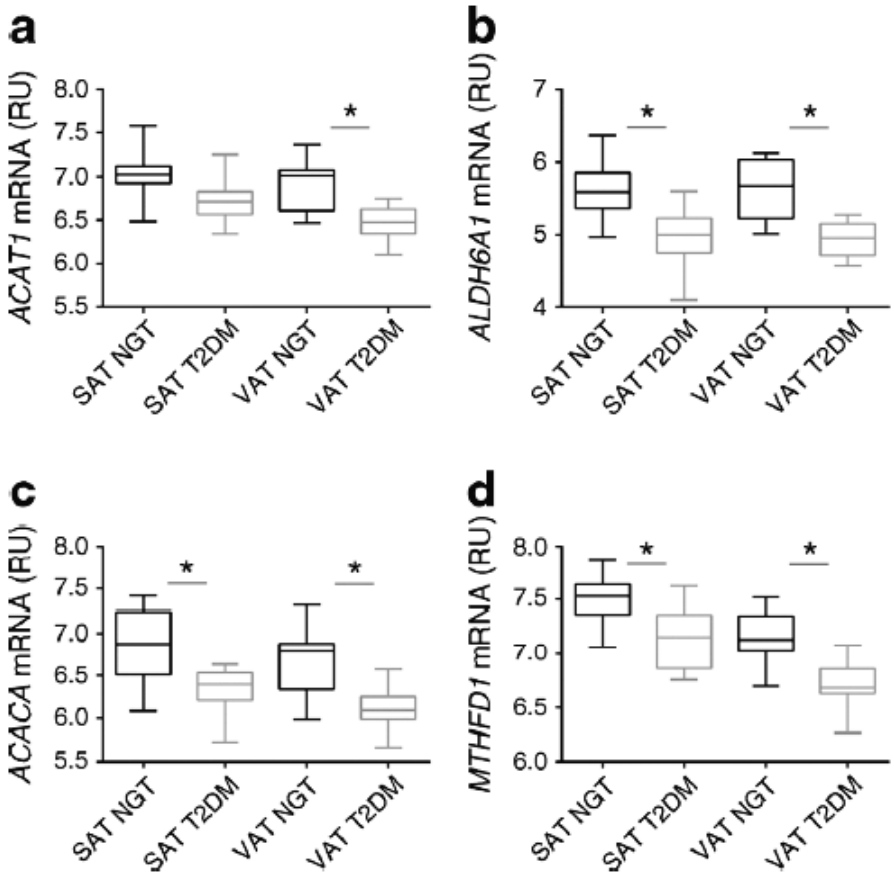

Figure 2 Gene expression of acetyl-CoA network genes in VAT and SAT. Box plots of normalised gene expression profiles (relative units [RU]: log2-scale) of a few representative genes, ACAT1 (a), ALDH6A1 (b), ACACA (c), MTHFD1 (d), in the acetyl-CoA reaction network that are downregulated (*adjusted p value <0.05 for indicated comparison) in both VAT and SAT of obese individuals with type 2 diabetes (grey bars) compared with NGT (black bars). The whiskers in the boxplots represent the upper and lower limits of the data. T2DM, type 2 diabetes

Down-regulation of genes in the acetyl-CoA reaction network recovers after weight loss

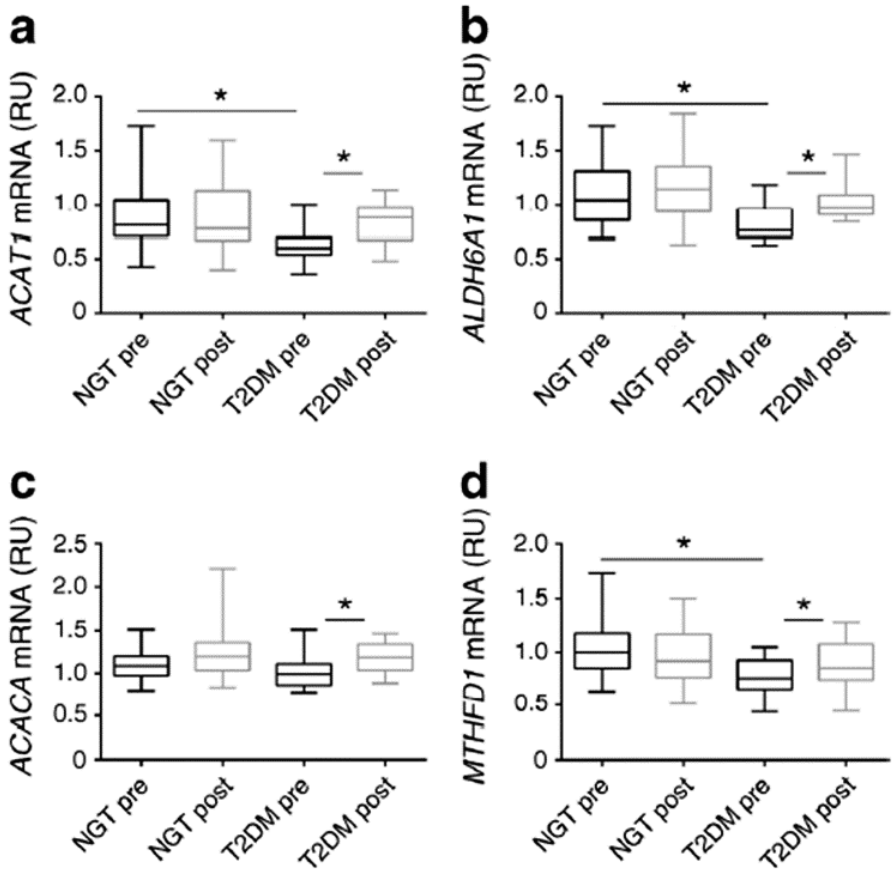

Figure 3 Gene expression of acetyl-CoA network genes in obese individuals with type 2 diabetes are normalised after bariatric surgery. Box plots of expression levels of four representative genes, ACAT1 (a), ALDH6A1 (b), ACACA (c), MTHFD1 (d) (as determined by quantitative PCR, corrected for housekeeping gene, linear scale: relative units [RU]), in type 2 diabetes and NGT before (black bars) and after bariatric surgery (grey bars). T2DM, type 2 diabetes. *p<0.05 (mixed-model-analysis). The whiskers in the boxplots represent the upper and lower limits of the data.

Among the 24 genes that overlapped between the statistically significant top hits in VAT and SAT, 9 genes are members of the acetyl-CoA gene set *(ACACA, ALDH6A1, MTHFD1, HADH, ME1, PC, LDHD, DHTKD1, and GNPAT)*. The gene expression profile of all the 9 genes from the RNA-Seq experiments shows a

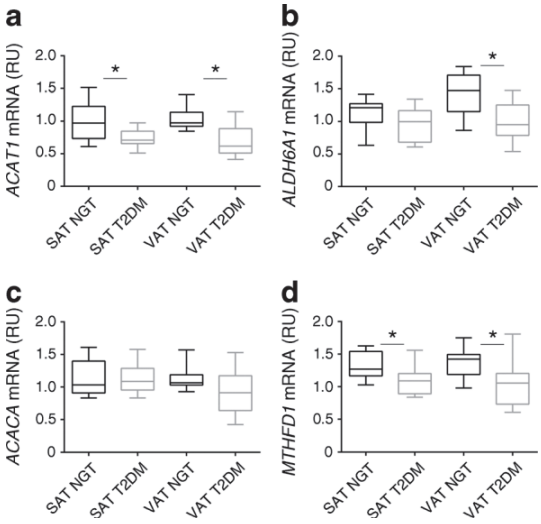

Figure 4 Gene expression of acetyl-CoA network genes in adipocytes. Adipocytes were isolated from SAT and VAT of individuals with type 2 diabetes (grey bars) and NGT (black bars). Gene expression of four representative genes, ACAT1 (a), ALDH6A1 (b), ACACA (c), MTHFD1 (d), was measured using quantitative PCR, corrected for housekeeping gene expression and plotted on a linear scale (RU). The whiskers in the boxplots represent the upper and lower limits of the data. T2DM, type 2 diabetes. *p<0.05 (t test) NGT vs T2DM

consistent down-regulation among individuals with type 2 diabetes in both adipose tissues. The boxplot depicting the expression levels in each of the tissues for both health types is shown for some of the acetyl-CoA genes in Figure 2.

To ascertain whether the down-regulation of the acetyl-CoA genes was correlated to type 2 diabetes, we compared the pre and post-surgery (3 months after) expression levels of these genes in SAT by qPCR. At this time the majority of diabetic obese women had a significantly improved metabolic health status as evidenced by lower fasting glucose levels (Table 1). We observed a statistically significant up-regulation of acetyl-CoA carboxylase alpha (*ACACA*) (p=9.3E-03), aldehyde dehydrogenase 6 family, member A1 (*ALDH6A1*) (p=4.1E-05) and methylenetetrahydrofolate dehydrogenase (*MTHFD1*) (p=4.7E-02) post-surgery in individuals with type 2 diabetes when compared with the changes in expression level observed in individuals with NGT (Fig 3). Also acetyl-CoA acetyltransferase 1 (*ACAT1*) which is at the

intersection of the acetyl-CoA network (Fig 1) was up-regulated post-surgery in type 2 diabetes (p=2.3E-03). Three other genes, encoding dehydrogenase E1 and transketolase domain (*DHTKD1*), lactate dehydrogenase (*LDHD*) and pyruvate carboxylase (*PC*) displayed a similar up-regulation post-surgery among individuals with type 2 diabetes but did not reach the statistical p-value threshold of 0.05. This indicates that the improved health status of diabetic individuals post-surgery is associated with a reversal of the disturbance in the acetyl-CoA metabolic network.

Gene expression of acetyl-CoA network in isolated adipocytes

As adipose tissue not only consists of adipocytes but is a mixture of cells, including endothelial cells and leukocytes we determined whether the down-regulation of the acetyl-CoA network in diabetic individuals specifically takes place in the adipocytes of the diabetic individuals. Indeed isolated adipocytes of diabetic individuals showed reduced gene expression levels for *ALDH6A1, ACAT1* and *MTHFD1* (Figure 4).

DISCUSSION

We have performed an in depth comparison of gene expression in SAT and VAT of severely obese women with and without type 2 diabetes. Network analyses revealed that the acetyl-CoA network was dysregulated in type 2 diabetes and that specific genes directly associated with acetyl-CoA metabolism were down-regulated in both VAT and SAT. Importantly, upon weight loss and amelioration of metabolic abnormalities, the expression of these genes in SAT recovered to the corresponding level among NGT women. These results imply that down-regulation of the acetyl-CoA network in VAT and SAT is a marker for the metabolic dysregulation characteristic of type 2 diabetes and, moreover, that it is reversible.

Network-based approaches have emerged as a powerful tool to unravel the mechanisms underlying complex traits [17-19]. Biological networks consist of molecular entities called nodes and functional interconnections between them called edges. An important property of these networks is that they are “scale-free” in that some nodes called “hubs” are connected to a substantially large number of other nodes and therefore considered essential for maintaining the integrity of the cell [18]. In general, these systems are robust against random mutations but are vulnerable to attacks against the hub [17]. Acetyl-CoA is a key hub metabolite of the metabolic network and plays a critical role in maintaining cellular homeostasis [20]. Previous studies have implicated branched-chain amino acid degradation (BCAD) [21], fatty-

acid oxidation [22, 23], and citrate cycle [22, 23] dysregulation as a characteristic feature of type 2 diabetes and related traits. In this study, in addition to confirming the previous findings, we argue that the acetyl-CoA reaction network is a unifying principle and that its dysregulation distinguishes between obese women with type 2 diabetes and those with NGT.

Acetyl-CoA lies at the crossroads of glycolysis, citrate cycle, ketogenesis, lipid synthesis, amino acid and fatty acid metabolism, suggesting that the metabolite may play a key role as an energy sensor in the cell [20]. Carbon skeletons of sugars, amino acids and fatty acids are degraded to the acetyl group to form acetyl-CoA that enters the citric acid cycle for energy generation. In addition, it is known to modulate gene expression through its role as a co-factor of histone acetyl-transferases (HAT) which enable the transcription of genes through histone acetylation at chromatin structures [24]. Cai et al argue that the primordial role of protein acetylation could have been to enable a cell to modulate gene expression/protein function in tune with the carbon source availability [25]. In other words, the acetyl-CoA is likely to serve as a fundamental and widely conserved gauge of metabolic state. A disturbance in this gauge may contribute to metabolic diseases such as type 2 diabetes as a consequence of altered cell metabolism and transcriptional regulation.

We report four genes associated with type 2 diabetes and recovery in the SAT of obese individuals: *ACAT1, ACACA*, *ALDH6A1* and *MTHFD1*. These genes all participate in the immediate vicinity of acetyl-CoA metabolism and are known hotspots of human metabolism, with *ACAT1*, *ALDH6A1* and *ACACA* recorded among inborn errors of metabolism (IEM) (OMIM: 203750, 614105 613933 respectively). IEMs are congenital metabolic defects arising due to single or multiple enzyme deficiencies. Recently [26], IEMs have been mapped onto a mathematical reconstruction of human metabolism [27]. Analyses of IEMs in the context of network topology led to the observation that the IEMs are adjacent to each other with acetyl-CoA acting as the central metabolite. This clearly suggests that the vicinity of acetyl-CoA in the network topology is a hub where abnormalities in individual genes potentially accumulate and upon reaching a certain risk threshold lead to the manifestation of disease.

The genes reported in this study function at critical decision points in cellular biochemical pathways as illustrated by *ACAT1.* The latter enzyme mediates the reversible conversion of 2 molecules of acetyl-CoA to acetoacetyl-CoA

[28]. This enzyme catalyzes the final step in branched-chain amino acid and fatty acid degradation pathways and the acetyl-CoA produced here is used as an input for the citric acid cycle (http://www.genome.jp/dbget-bin/www_bget?hsa:38). When energetics favors the production of acetoacetyl-CoA in this reaction step, the metabolite is used for ketone body synthesis [28]. *ACAT1* also mediates the first step in the mevalonate pathway whose end-product Farnesyl-PP is a precursor for cholesterol among other several important metabolites (http://www.genome.jp/dbget-bin/www_bget?hsa:38). Therefore, the *ACAT1* enzyme is strategically placed at the intersection of important cellular pathways that respond to the energy status of the cell.

Intriguingly, additional genetic evidence for a role of *ACAT1* in type 2 diabetes is provided by a genome-wide association study (GWAS) in a UK prospective diabetes study that investigated the glycemic response to metformin and reported a Single Nucleotide Polymorphism (SNP), rs11212617, associated with metformin success [29]. Based on the proximity to the polymorphism, the study concluded *ATM* (ataxia telangiectasia mutated) as the causal gene that plays a role in metformin success and that the variation at this gene alters the glycemic response to metformin. However, re-analyzing the polymorphism rs11212617, we found that the polymorphism is in fact an eQTL for the nearby *ACAT1* gene and not *ATM*. The confirmation for this eQTL is provided by two independent studies; Zeller et al who studied the monocyte transcriptome to determine eQTLs of relevance to human disease [31] (http://eqtl.uchicago.edu/cgi-bin/gbrowse/eqtl/) and the data from the GEUVADIS consortium [31, 32], where the SNP was found to be an eQTL for *ACAT1* (nominal p-value=1.1e-6). This means that the variation in the expression level of *ACAT1* alters the glycemic response to metformin and therefore plays a role in the success of metformin treatment. Furthermore, this clearly suggests that *ACAT1* plays a role in type 2 diabetes. Individuals with the polymorphism that alters its expression level may represent a sub-type among individuals with type 2 diabetes, perhaps with different response to metformin.

There were differences in the usage of medication between obese women NGT and type 2 diabetes, especially in the usage of metformin, which was not used by any of the NGT women and by 60% of the women with type 2 diabetes. As metformin acts on enzymes within the acetyl-coA network and affects lipid and glucose metabolism, the usage of metformin may have confounded our results, but we have not found any evidence for this: 1) There was no difference in gene expression of *ACAT1*, *ALDH6A1*, *ACACA* and

MTHFD1 between metformin and no metformin users (ESM Fig. 1). 2) When metformin users were excluded from the comparison between individuals with NGT and those with type 2 diabetes, there was still a down-regulation of *ACAT1*, *ALDH6A1*, *ACACA* and *MTHFD1* in the women with type 2 diabetes (ESM Fig. 2).

Our cohort consisted of severely obese women. We do not know whether the observed differences were a consequence of the metabolic defects that occur in type 2 diabetes (i.e. hyperglycemia) or represented the underlying etiology of type 2 diabetes. However, a previous study that used microarrays to analyse gene expression in adipose tissue showed that during the progression from the lean to the obese state and then further towards the metabolic syndrome the genes involved in metabolic processing were gradually down-regulated [10]. These data suggest that the down-regulation of metabolic pathways underlie the pathology of type 2 diabetes.

Previous studies have postulated that low-grade inflammation of the adipose tissue plays an important role in the development of insulin resistance [33-36]. For example, a recent study in monozygotic twins discordant for obesity showed that SAT transcript profile in the metabolically healthy obese is characterized by the maintenance of mitochondrial function and absence of inflammation [35]. This is in line with the results in our study, where we observe an inverse correlation pattern of differential expression of genes that are down-regulated in metabolic and up-regulated in inflammatory pathways in VAT and SAT of individuals with type 2 diabetes.

In summary, our results demonstrate that the acetyl-CoA network is dysregulated in VAT and SAT of obese women with type 2 diabetes. We find significant down-regulation of several genes in the immediate vicinity of acetyl-CoA and report a statistically significant recovery for 4 genes after amelioration of the metabolic abnormalities in SAT. Further research into the causal role of down-regulation of the acetyl-CoA network in type 2 diabetes should indicate whether direct intervention in the acetyl-CoA network will provide novel therapeutic approaches.

References

1. Malik VS, Willett WC, Hu FB: **Global obesity: trends, risk factors and policy implications.** *Nat Rev Endocrinol* 2013, **9**:13–27.

2. Mokdad AH, Ford ES, Bowman BA, Dietz WH, Vinicor F, Bales VS, Marks JS: **Prevalence of obesity, diabetes, and obesity-related health risk factors, 2001**. *JAMA : the journal of the American Medical Association* 2003, **289**(1):76-79.

3. Van Gaal LF, Mertens IL, De Block CE: **Mechanisms linking obesity with cardiovascular disease**. *Nature* 2006, **444**(7121):875-880.

4. Bluher M: **Are there still healthy obese patients?** *Current opinion in endocrinology, diabetes, and obesity* 2012, **19**(5):341-346.

5. Bluher M: **Adipose tissue dysfunction contributes to obesity related metabolic diseases**. *Best practice & research Clinical endocrinology & metabolism* 2013, **27**(2):163-177.

6. Kantartzis K, Machann J, Schick F, Rittig K, Machicao F, Fritsche A, Haring HU, Stefan N: **Effects of a lifestyle intervention in metabolically benign and malign obesity**. *Diabetologia* 2011, **54**(4):864-868.

7. Lindstrom J, Tuomilehto J: **The diabetes risk score: a practical tool to predict type 2 diabetes risk**. *Diabetes care* 2003, **26**(3):725-731.

8. Pajunen P, Kotronen A, Korpi-Hyovalti E, Keinanen-Kiukaanniemi S, Oksa H, Niskanen L, Saaristo T, Saltevo JT, Sundvall J, Vanhala M *et al*: **Metabolically healthy and unhealthy obesity phenotypes in the general population: the FIN-D2D Survey**. *BMC public health* 2011, **11**:754.

9. Wolfs MG, Rensen SS, Bruin-Van Dijk EJ, Verdam FJ, Greve JW, Sanjabi B, Bruinenberg M, Wijmenga C, van Haeften TW, Buurman WA *et al*: **Co-expressed immune and metabolic genes in visceral and subcutaneous adipose tissue from severely obese individuals are associated with plasma HDL and glucose levels: a microarray study**. *BMC medical genomics* 2010, **3**:34.

10. Klimčáková E, Roussel B, Márquez-Quiñones A, Kováčová Z, Kováčiková M, Combes M, Šiklová-Vítková M, Hejnová J, Šrámková P, Bouloumié A, Viguerie N, Štich V, Langin D: **Worsening of obesity and metabolic status yields similar molecular adaptations in human subcutaneous and visceral adipose tissue: Decreased metabolism and increased immune response**. *J Clin Endocrinol Metab* 2011, **96**.

11. Qatanani M, Tan Y, Dobrin R, Greenawalt DM, Hu G, Zhao W, Olefsky JM, Sears DD, Kaplan LM, Kemp DM: **Inverse regulation of inflammation and mitochondrial function in adipose tissue defines extreme insulin sensitivity in morbidly obese patients**. *Diabetes* 2013, **62**:855–863.

12. Mortazavi A, Williams BA, McCue K, Schaeffer L, Wold B: **Mapping and quantifying mammalian transcriptomes by RNA-Seq**. *Nature methods* 2008, **5**(7):621-628.

13. Ozsolak F, Milos PM: **RNA sequencing: advances, challenges and opportunities**. *Nature reviews Genetics* 2011, **12**(2):87-98.

14. Wang Z, Gerstein M, Snyder M: **RNA-Seq: a revolutionary tool for transcriptomics**. *Nature reviews Genetics* 2009, **10**(1):57-63.

15. Van Harmelen V, Lonnqvist F, Thorne A, Wennlund A, Large V, Reynisdottir S, Arner P: **Noradrenaline-induced lipolysis in isolated mesenteric, omental and subcutaneous adipocytes from obese subjects**. *International journal of obesity and related metabolic disorders : journal of the International Association for the Study of Obesity* 1997, **21**(11):972-979.

16. Goeman JJ, van de Geer SA, de Kort F, van Houwelingen HC: **A global test for groups of genes: testing association with a clinical outcome**. *Bioinformatics* 2004, **20**(1):93-99.

17. Barabasi AL, Gulbahce N, Loscalzo J: **Network medicine: a network-based approach to human disease**. *Nature reviews Genetics* 2011, **12**(1):56-68.

18. Liu M, Liberzon A, Kong SW, Lai WR, Park PJ, Kohane IS, Kasif S: **Network-based analysis of affected biological processes in type 2 diabetes models**. *PLoS genetics* 2007, **3**(6):e96.

19. Chan SY, Loscalzo J: **The emerging paradigm of network medicine in the study of human disease**. *Circulation research* 2012, **111**(3):359-374.

20. Naimi M, Arous C, Van Obberghen E: **Energetic cell sensors: a key to metabolic homeostasis**. *Trends in endocrinology and metabolism: TEM* 2010, **21**(2):75-82.

21. Herman MA, She P, Peroni OD, Lynch CJ, Kahn BB: **Adipose tissue branched chain amino acid (BCAA) metabolism modulates circulating BCAA levels**. *The Journal of biological chemistry* 2010, **285**(15):11348-11356.

22. Dahlman I, Forsgren M, Sjogren A, Nordstrom EA, Kaaman M, Naslund E, Attersand A, Arner P: **Downregulation of electron transport chain genes in visceral adipose tissue in type 2 diabetes independent of obesity and possibly involving tumor necrosis factor-alpha**. *Diabetes* 2006, **55**(6):1792-1799.

23. Dahlman I, Mejhert N, Linder K, Agustsson T, Mutch DM, Kulyte A, Isaksson B, Permert J, Petrovic N, Nedergaard J *et al*: **Adipose tissue pathways involved in weight loss of cancer cachexia**. *British journal of cancer* 2010, **102**(10):1541-1548.

24. Cai L, Sutter BM, Li B, Tu BP: **Acetyl-CoA induces cell growth and proliferation by promoting the acetylation of histones at growth genes**. *Molecular cell* 2011, **42**(4):426-437.

25. Cai L, Tu BP: **On acetyl-CoA as a gauge of cellular metabolic state**. *Cold Spring Harbor symposia on quantitative biology* 2011, **76**:195-202.

26. Sahoo S, Franzson L, Jonsson JJ, Thiele I: **A compendium of inborn errors of metabolism mapped onto the human metabolic network**. *Molecular bioSystems* 2012, **8**(10):2545-2558.

27. Thiele I, Swainston N, Fleming RM, Hoppe A, Sahoo S, Aurich MK, Haraldsdottir H, Mo ML, Rolfsson O, Stobbe MD *et al*: **A community-driven global reconstruction of human metabolism**. *Nature biotechnology* 2013, **31**(5):419-425.

28. Haapalainen AM, Merilainen G, Pirila PL, Kondo N, Fukao T, Wierenga RK: **Crystallographic and kinetic studies of human mitochondrial acetoacetyl-CoA thiolase: the importance of potassium and chloride ions for its structure and function**. *Biochemistry* 2007, **46**(14):4305-4321.

29. GoDarts, Group UDPS, Wellcome Trust Case Control C, Zhou K, Bellenguez C, Spencer CC, Bennett AJ, Coleman RL, Tavendale R, Hawley SA *et al*: **Common variants near ATM are associated with glycemic response to metformin in type 2 diabetes**. *Nature genetics* 2011, **43**(2):117-120.

30. Zeller T, Wild P, Szymczak S, Rotival M, Schillert A, Castagne R, Maouche S, Germain M, Lackner K, Rossmann H *et al*: **Genetics and beyond--the transcriptome of human monocytes and disease susceptibility**. *PloS one* 2010, **5**(5):e10693.

31. Lappalainen T, Sammeth M, Friedlander MR, t Hoen PA, Monlong J, Rivas MA, Gonzalez-Porta M, Kurbatova N, Griebel T, Ferreira PG *et al*: **Transcriptome and genome sequencing uncovers functional variation in humans**. *Nature* 2013, **501**(7468):506-511.

32. t Hoen PA, Friedlander MR, Almlof J, Sammeth M, Pulyakhina I, Anvar SY, Laros JF, Buermans HP, Karlberg O, Brannvall M *et al*: **Reproducibility of high-throughput mRNA and small RNA sequencing across laboratories**. *Nature biotechnology* 2013, **31**(11):1015-1022.

33. Soronen J, Laurila PP, Naukkarinen J, Surakka I, Ripatti S, Jauhiainen M, Olkkonen VM, Yki-Jarvinen H: **Adipose tissue gene expression analysis reveals changes in inflammatory, mitochondrial respiratory and lipid metabolic pathways in obese insulin-resistant subjects**. *BMC medical genomics* 2012, **5**:9.

34. Karelis AD, Faraj M, Bastard JP, St-Pierre DH, Brochu M, Prud'homme D, Rabasa-Lhoret R: **The metabolically healthy but obese individual presents a favorable inflammation profile**. *The Journal of clinical endocrinology and metabolism* 2005, **90**(7):4145-4150.

35. Naukkarinen J, Heinonen S, Hakkarainen A, Lundbom J, Vuolteenaho K, Saarinen L, Hautaniemi S, Rodriguez A, Fruhbeck G, Pajunen P *et al*: **Characterising metabolically healthy obesity in weight-discordant monozygotic twins**. *Diabetologia* 2014, **57**(1):167-176.

36. Phillips CM, Perry IJ: **Does inflammation determine metabolic health status in obese and nonobese adults?** *The Journal of clinical endocrinology and metabolism* 2013, **98**(10):E1610-1619.

Supplementary Section

ESM Methods 1: Methods describing RNA deep sequencing, Alignment and Gene annotation and Differential Gene Expression Analysis

RNA Deep Sequencing

The experimental pipeline followed by BGI consisted of enriching mRNA with the help of oligo(dT) beads. Fragmentation buffer was added to generate short mRNA fragments. Taking these short fragments as templates, random hexamer primers were used to synthesize the first strand cDNA. The second strand cDNA was synthesized using buffer, dNTPs, RNase H and DNA polymerase I. Short fragments were purified with QiaQuick PCR extraction kit and resolved with EB-buffer for end reparation and adding poly(A). The short fragments were then connected with sequencing adaptors. Suitable fragments were then selected for amplification by PCR.

Alignment and gene annotation

After assessing the quality of the raw data using FastQC, version: 0.9.3 (http://www.bioinformatics.babraham.ac.uk/projects/fastqc/), we aligned the reads to the Human reference genome build 19 (hg19, GRCh37) using GSNAP [1] with the novel splicing option (-N1) enabled. The aligned data was further converted to a sorted BAM file using SAMTools, version: 0.1.18 [2]. For the quantification of the number of nucleotides that were mapped per exon, we used BEDTools, version: 2.13.2 [3] in conjunction with an in-house program (https://git.lumc.nl/lgtc-bioinformatics/ngs-misc/blob/master/src/hist2count.py) to obtain a histogram of coverage per exon and the associated count data. Gene annotation (RefSeq version v54) was retrieved from the UCSC (http://genome.ucsc.edu/cgi-bin/hgTables?db=hg19, retrieved July 9, 2012).

Differential Gene Expression

Differential expression analysis was done on exon, gene and transcript levels. For exon level analyses, we summed the coverage values of all nucleotides in an exon for all unique exons annotated in Ensembl. For transcript and gene level analysis, the coverage in all exonic regions of a transcript gene were summed. Only genes expressed in 75% or more of the samples were retained in the statistical analysis as a filter for low abundant genes. To account for differences in number or reads per sample, count data were normalized with the TMM function from the edgeR package [4]. Data were log-transformed with the voom function from the limma-package

[5]. Weights from the voom transformation were taken into subsequent linear models. A hierarchical linear model was fit with the voom transformed expression data as dependent variables and health status and tissue as the independent variables, using the lmFit function from the limma package. P-values were corrected for multiple testing using Benjamini-Hochberg false discovery rate. Entrez Gene identifiers were retrieved using the biomaRt package v2.12.0 in R.

ESM Methods 2: Bioinformatic analysis to identify sub-networks in gene expression data

Bioinformatic visualization tools

Over-representation analysis tools made available by ConsensusPathDB (http://cpdb.molgen.mpg.de/) were used to investigate the relationship among top differentially expressed genes in VAT and SAT. To determine if significantly differentially expressed genes in each of the two tissues operate in close proximity in network space, we utilized "Network neighbourhood-based entity sets" (NEST).

Acetyl-CoA gene set generation

The Taverna version 2.4 [6] workflow management system was used to generate the gene set for acetyl-CoA. We employed a reaction scheme [7] that can be visualized as expanding by a radius of 2 steps in the reaction space of acetyl-CoA. Specifically in this scheme, the reactions that acetyl-CoA is part of and the compounds that participate in these reactions is determined using information present in the KEGG-database [release 63] [8]. As an intermediate step certain compounds like ATP, ADP, NADP, NADPH were filtered out in order to avoid non-specific connections.

Global test

Global test is a statistical method to determine if global expression pattern of a group of genes is significantly related to the phenotype of interest. The global test is available as an R-package at http://www.bioconductor.org/packages/2.13/bioc/html/globaltest.html.
The voom-transformed gene expression data as mentioned earlier was used to determine the association of all the genes as well as to evaluate the association of the acetyl-CoA gene set with T2DM.

ESM Methods 3: Quantitative Real Time PCR for comparison of pre and post-surgery gene expression data for select members of acetyl-CoA gene set

The RNA of the needle biopsies obtained pre and post bariatric surgery as well as the RNA obtained from the adipocytes during bariatric surgery were used for quantitative real-time PCR. Six hundred ng of total RNA was reverse-transcribed with iScript cDNA synthesis kit (Bio-Rad, Hercules, CA) and obtained cDNA was purified with Nucleospin Extract II kit (Macherey-Nagel). Real-Time PCR was carried out on the IQ5 PCR machine (Biorad) using the Sensimix SYBR Green RT-PCR mix (Quantace, London, UK) and QuantiTect SYBR Green RT-PCR mix (Qiagen, Valencia, CA). mRNA levels were calculated and normalized to mRNA levels of the housekeeping gene *LRP10* using Bio-Rad CFX Manager 3.0 software (Bio-Rad). Primer sequences are listed in ESM Table 1.

ESM Methods 4: Reaction Scheme implemented in Taverna, a workflow management system.

Genes within two reaction steps of acetyl coA are identified in the KEGG pathway database. These form the gene set for acetyl coA metabolism. The method is shown in the workflow below and further discussed in Dharuri et al[7].

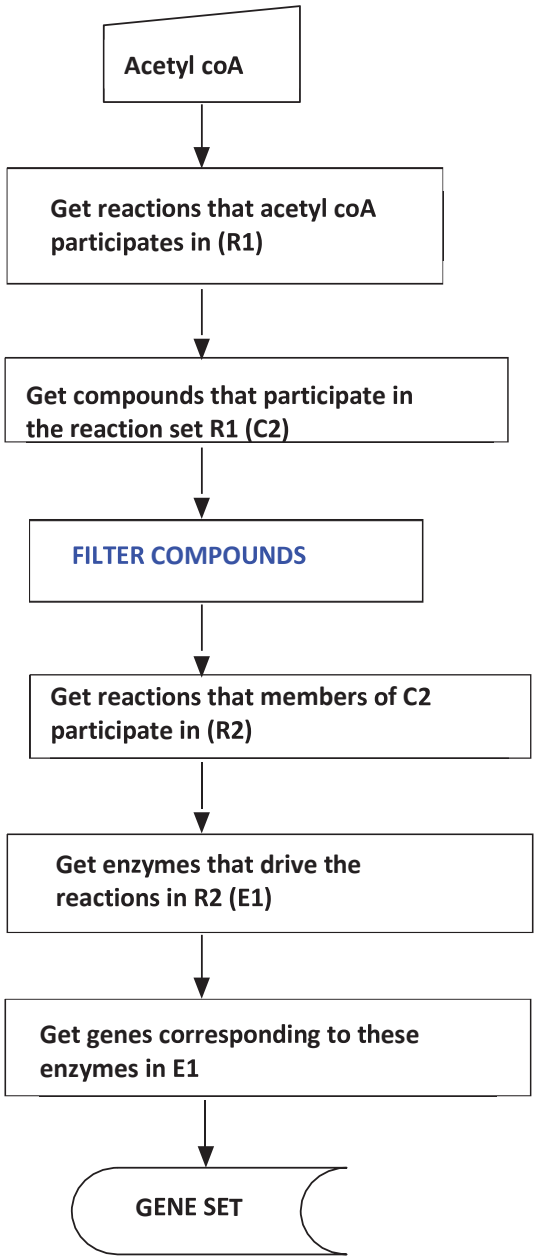
Acetyl coA
Get reactions that acetyl coA participates in (R1)
Get compounds that participate in the reaction set R1 (C2)
FILTER COMPOUNDS
Get reactions that members of C2 participate in (R2)
Get enzymes that drive the reactions in R2 (E1)
Get genes corresponding to these enzymes in E1
GENE SET

ESM Table 1: Sequences of primers used in the qPCR

Gene	Fw primer	Rv primer	Annealing Temperature
LRP10	CAGACTGTCACCATCAGGTTC	GAGAGGGGAGCGTAGGGTTA	60
ACACA	TTTAAGGGGTGAAGAGGGTGC	CCAGAAAGACCTAGCCCTCAAG	56
ACAT1	CAATTGGGATGTCTGGAGC	TAGCATGGCAGAAGCACCTC	58
ALDH6A1	GTGCTTCTGGGCAGTAGAG	TCACCTTGGAAGAAACCTGC	58
MTHFD1	AGGTGTCCCTACAGGCTTCA	GCATTGTGCTCATCGTTCCT	61

ESM Table 2: Genes significantly up or down-regulated in VAT of T2DM subjects

gene_id	Coefficient VAT NGT vs T2DM	p- value VAT NGT vs T2DM	p-value adj VAT NGTvs T2DM	Coefficient SAT NGTvs T2DM	p-value SAT NGT vs T2DM	p-value adj SAT NGTvs T2DM
ALDH6A1	-0.67033	1.49E-06	0.005502	-0.59541	5.12E-05	0.042281
C14orf45	-0.46222	1.59E-06	0.005502	-0.39723	0.000107	0.042281
ECHS1	-0.52103	1.48E-06	0.005502	-0.31088	0.003448	0.078286
IRS1	-0.6011	3.41E-07	0.005502	-0.64306	7.26E-06	0.027696
STBD1	-0.61468	6.74E-07	0.005502	-0.32893	0.005018	0.089566
IARS2	-0.31061	2.73E-06	0.006958	-0.18008	0.001517	0.060769
NAT8L	-0.74468	2.81E-06	0.006958	-0.44867	0.001498	0.060769
AIFM2	-0.45243	3.24E-06	0.007013	-0.24872	0.002298	0.070283
ATPAF1	-0.34906	3.71E-06	0.007141	-0.29532	0.003426	0.078286
ACAD9	-0.31106	8.28E-06	0.010501	-0.26532	0.001228	0.0603
GPI	-0.28503	8.25E-06	0.010501	-0.16923	0.008524	0.10884
HADH	-0.57479	8.49E-06	0.010501	-0.45138	0.000145	0.042281
HSPD1	-0.29857	7.74E-06	0.010501	-0.16624	0.029418	0.183414
MTHFD1	-0.42341	6.16E-06	0.010501	-0.3727	7.95E-05	0.042281
ACACA	-0.56009	9.14E-06	0.010554	-0.47629	0.000297	0.0487
MAP3K15	-0.43265	1.19E-05	0.012882	-0.39465	9.36E-05	0.042281
HK2	-0.71165	1.32E-05	0.01298	-0.38422	0.005958	0.094515
PARVG	0.654257	1.5E-05	0.01298	0.744737	0.000608	0.055969
PDHA1	-0.37534	1.48E-05	0.01298	-0.28852	0.001045	0.057525
PRKAR2B	-0.71637	1.39E-05	0.01298	-0.37036	0.02795	0.179313
ACAT1	-0.4062	1.81E-05	0.012994	-0.27406	0.002336	0.070807
ATP9A	-0.40037	2.1E-05	0.012994	-0.34628	0.005481	0.091691
CEBPA	-0.5664	1.97E-05	0.012994	-0.37387	0.002787	0.075329

DARS2	-0.37947	1.64E-05	0.012994	-0.30113	0.000532	0.055836
NXPH4	-1.0023	1.89E-05	0.012994	-0.72237	0.039951	0.213164
OXCT1	-0.5273	1.99E-05	0.012994	-0.41823	0.000444	0.053704
SLC2A4	-0.88429	2.09E-05	0.012994	-0.73171	0.000105	0.042281
TMEM120B	-0.39756	2.09E-05	0.012994	-0.40465	0.001103	0.058403
HIBADH	-0.34092	2.41E-05	0.014395	-0.2844	0.00054	0.055836
MME	-0.87028	2.53E-05	0.014586	-0.24391	0.077446	0.290709
ATP5B	-0.29223	2.73E-05	0.014753	-0.14885	0.01547	0.136867
CST7	0.804504	2.9E-05	0.014753	0.57403	0.009737	0.114841
GPT2	-0.59523	2.68E-05	0.014753	-0.4677	0.000991	0.057525
UQCRC2	-0.3105	2.85E-05	0.014753	-0.18736	0.001774	0.064807
PHYH	-0.4099	3.1E-05	0.015179	-0.25588	0.002172	0.068621
SORBS1	-0.52573	3.16E-05	0.015179	-0.3601	0.002971	0.076138
FXYD5	0.462931	3.38E-05	0.015638	0.508216	3E-05	0.041435
ME1	-0.44801	3.52E-05	0.015638	-0.45845	9.99E-05	0.042281
SDHC	-0.32374	3.52E-05	0.015638	-0.20976	0.009145	0.111578
LOC401052	-0.5606	3.92E-05	0.016969	-0.46015	0.003091	0.076138
ABHD14A-	-0.31203	4.04E-05	0.017066	-0.12479	0.067336	0.274133
CS	-0.40868	4.37E-05	0.017595	-0.25358	0.003252	0.07663
FASN	-0.86173	4.3E-05	0.017595	-0.709	0.000487	0.055836
PECR	-0.52655	4.55E-05	0.017913	-0.39495	0.002181	0.068769
LOC80054	-0.5741	4.98E-05	0.018747	-0.36113	0.006328	0.096929
NEK9	-0.24342	4.92E-05	0.018747	-0.25243	0.000163	0.043349
ADCY6	-0.39224	5.76E-05	0.018983	-0.34851	0.001307	0.060323
CDO1	-0.60039	5.76E-05	0.018983	-0.34148	0.013689	0.128261
DMGDH	-0.51115	5.65E-05	0.018983	-0.39788	0.001753	0.064445
GCOM1	-0.42785	5.8E-05	0.018983	-0.2221	0.020122	0.156278

KCNN4	0.791172	5.35E-05	0.018983	0.719036	0.004726	0.087804
LETMD1	-0.31904	5.81E-05	0.018983	-0.21855	0.002345	0.070845
PEX19	-0.34994	5.62E-05	0.018983	-0.30875	0.000527	0.055836
MLXIPL	-0.47102	6.33E-05	0.019469	-0.39568	0.00155	0.060769
MUT	-0.36496	6.25E-05	0.019469	-0.29517	0.000441	0.053704
NDUFS1	-0.33767	6.41E-05	0.019469	-0.26825	0.005722	0.092817
PC	-0.51421	6.25E-05	0.019469	-0.33894	0.000302	0.0487
ATP5A1	-0.26726	6.8E-05	0.020287	-0.15425	0.012799	0.125416
FNTA	-0.23067	7.3E-05	0.021412	-0.15997	0.000901	0.057525
GYG2	-0.49552	7.54E-05	0.021771	-0.37986	0.000567	0.055836
C12orf35	0.482851	8.21E-05	0.022143	0.211704	0.110692	0.347015
LDHD	-0.7308	7.85E-05	0.022143	-0.53027	9.59E-05	0.042281
MCCC1	-0.44783	8.31E-05	0.022143	-0.32769	0.002073	0.067862
MYOM1	-0.74875	7.95E-05	0.022143	-0.57005	0.001222	0.0603
SLC25A33	-0.55683	8.31E-05	0.022143	-0.21109	0.106244	0.340839
CD3D	1.057606	9.32E-05	0.024452	0.689572	0.015962	0.139
ITGA7	-0.43821	9.49E-05	0.024532	-0.29145	0.000602	0.055969
HADHB	-0.28151	9.67E-05	0.024621	-0.12942	0.071027	0.280078
FAH	-0.36888	0.000102	0.025337	-0.21549	0.015303	0.136221
PGM1	-0.43899	0.000102	0.025337	-0.32841	0.006897	0.100804
FAN1	-0.24678	0.000104	0.025465	-0.26323	5.17E-05	0.042281
MYZAP	-0.49368	0.00011	0.026527	-0.31503	0.002982	0.076138
MGEA5	-0.34359	0.000114	0.026968	-0.30296	0.001829	0.065041
ALDH2	-0.47219	0.000126	0.027353	-0.40667	0.001386	0.060323
FBXO27	-0.47275	0.00012	0.027353	-0.32289	0.006789	0.100256
KCNIP2	-0.57813	0.000126	0.027353	-0.33357	0.026098	0.174084
PDHX	-0.3518	0.000117	0.027353	-0.25083	0.005747	0.092817
PFKFB1	-0.61156	0.000124	0.027353	-0.57186	0.00039	0.051411
SLC6A6	0.448635	0.000126	0.027353	0.388987	0.020459	0.157549

TM7SF2	-0.65447	0.000121	0.027353	-0.5652	0.000245	0.048507
DLD	-0.36203	0.00013	0.027768	-0.22936	0.002916	0.075807
PEX11A	-0.54283	0.000134	0.028208	-0.28022	0.029285	0.18285
ALDH5A1	-0.41815	0.000143	0.028227	-0.37903	0.002663	0.074601
BNIP3	-0.46674	0.000136	0.028227	-0.26732	0.005206	0.090496
CPS1	-0.592	0.000147	0.028227	-0.45495	0.002242	0.069444
FH	-0.25037	0.00014	0.028227	-0.08348	0.209234	0.476835
GABRE	-0.41347	0.00014	0.028227	-0.44716	0.00082	0.056752
LETM1	-0.28644	0.000144	0.028227	-0.15596	0.025489	0.17185
PCCB	-0.39374	0.000144	0.028227	-0.19472	0.022988	0.165424
PHF13	-0.39433	0.000147	0.028227	0.050692	0.625383	0.816692
ARG2	-0.29061	0.000149	0.028265	-0.14506	0.020686	0.158062
BTBD6	-0.40376	0.00015	0.028313	-0.22028	0.015406	0.136581
CA8	-0.72509	0.000153	0.028427	-0.52113	0.011228	0.120415
LST1	0.597583	0.000156	0.028427	0.73995	0.000566	0.055836
YWHAG	-0.34916	0.000156	0.028427	-0.1706	0.053963	0.247066
APCDD1	-0.43512	0.000159	0.028617	-0.20187	0.148309	0.399287
ETFDH	-0.36711	0.000161	0.02868	-0.20541	0.008033	0.106776
MMD	-0.62533	0.000165	0.029125	-0.41409	0.003817	0.082012
AMICA1	0.708154	0.00017	0.029539	0.760944	0.00161	0.061115
OGDH	-0.21233	0.000171	0.029539	-0.12606	0.024143	0.168181
ACO1	-0.38915	0.000173	0.029635	-0.27544	0.000833	0.056752
ACOT1	-0.53314	0.000176	0.029652	-0.34982	0.007398	0.103802
COQ6	-0.30529	0.000178	0.029652	-0.23084	0.001309	0.060323
TUSC5	-0.39626	0.000178	0.029652	-0.31553	0.01315	0.126493
AIFM1	-0.25849	0.000182	0.02994	-0.12482	0.055699	0.250486
AKAP1	-0.45989	0.000183	0.02994	-0.22612	0.069932	0.278155
CAT	-0.33619	0.000193	0.031147	-0.25952	0.001106	0.058403
DLST	-0.24018	0.000195	0.031147	-0.08557	0.070547	0.278997

PLIN5	-0.77331	0.000196	0.031147	-0.6064	0.004128	0.084327
GLUD2	-0.2456	0.000205	0.032341	-0.11297	0.038981	0.211289
IMMT	-0.19286	0.000209	0.032599	-0.13107	0.006316	0.096929
PCCA	-0.38327	0.000211	0.032658	-0.30718	0.004828	0.088137
ACADS	-0.47336	0.000218	0.033182	-0.22351	0.012826	0.125416
CHST11	0.474785	0.000218	0.033182	0.587619	0.001251	0.060323
RETSAT	-0.45639	0.000221	0.033265	-0.28288	0.016783	0.142511
PDE3B	-0.53384	0.000231	0.034471	-0.31326	0.031749	0.189882
AKR1B10	4.423196	0.000239	0.034715	2.274977	0.094247	0.321015
BCL2L13	-0.2233	0.000243	0.034715	-0.09604	0.143732	0.393576
CHCHD10	-0.43065	0.000236	0.034715	-0.07441	0.439305	0.683267
DIS3L	-0.22639	0.00024	0.034715	-0.16482	0.026102	0.174084
ORMDL3	-0.3648	0.000241	0.034715	-0.35641	0.00098	0.057525
ADORA3	0.787044	0.000248	0.03485	0.849999	0.005258	0.090592
BOK	-0.5296	0.000248	0.03485	-0.42262	0.00056	0.055836
CORO1A	0.588905	0.000253	0.03485	0.57774	0.001825	0.065041
EPB41L4B	-0.5678	0.000254	0.03485	-0.39557	0.005131	0.0902
NDN	-0.29789	0.000253	0.03485	-0.14583	0.056384	0.251827
ACADM	-0.45711	0.000264	0.035079	-0.37292	0.002267	0.069893
ACADSB	-0.33375	0.000265	0.035079	-0.3195	0.000556	0.055836
ADSSL1	-0.75955	0.000259	0.035079	-0.67785	0.000229	0.048025
HSDL2	-0.33571	0.000262	0.035079	-0.24675	0.006545	0.098355
PHKA2	-0.30828	0.000259	0.035079	-0.35695	0.000548	0.055836
KLRK1	0.713466	0.000269	0.035309	0.429783	0.072961	0.283239
STRADB	-0.36152	0.000283	0.036577	-0.23321	0.032869	0.193406
TYRO3	-0.31518	0.000282	0.036577	-0.30272	0.003522	0.078997
CYB5A	-0.32699	0.000289	0.036589	-0.343	0.001823	0.065041
KIAA0368	-0.18082	0.00029	0.036589	-0.14045	0.020676	0.158062
PXMP2	-0.44048	0.000289	0.036589	-0.46718	1.65E-05	0.03571

ACOT2	-0.5115	0.000294	0.036657	-0.26945	0.03003	0.184965
C1orf162	0.679527	0.000292	0.036657	0.756212	0.000302	0.0487
UQCC	-0.26188	0.000297	0.036689	-0.25136	0.000325	0.048769
CD8B	1.149373	0.000323	0.039612	0.889473	0.031652	0.18956
HCAR1	-0.49796	0.000332	0.040514	-0.5247	0.023562	0.16643
HSD17B4	-0.19447	0.000345	0.041461	-0.12918	0.04775	0.231962
ZNF436	-0.33341	0.000343	0.041461	-0.01462	0.852844	0.93309
ADHFE1	-0.52698	0.000359	0.041829	-0.42806	0.0025	0.072607
MRPL30	-0.23547	0.000358	0.041829	-0.14517	0.014305	0.131674
PHLDB2	-0.37206	0.000354	0.041829	-0.29726	0.016369	0.140724
RRM1	-0.22802	0.000354	0.041829	-0.15169	0.044719	0.225816
TNS1	-0.42061	0.00036	0.041829	-0.35763	0.005129	0.0902
CENPK	1.086756	0.000365	0.042038	0.528342	0.076188	0.289028
KANK1	-0.39156	0.000367	0.042038	-0.29404	0.007223	0.102463

Coefficient VAT NGT vs T2DM: log fold change of NGT vs T2DM in visceral adipose tissue; a negative value reflects down-regulation whereas a positive value reflects up-regulation of the gene in T2DM subjects. Adj p-value NGT vs T2DM: p-value after Benjamin-Hochberg FDR correction. Also the log fold change and p-values for subcutaneous tissue (SAT) are shown. The genes highlighted in grey are the 42 genes that are members of the acetyl-CoA network. All these 42 genes are significantly down-regulated in VAT of T2DM.

ESM Table 3: KEGG Pathway over-representation analysis among significantly differentially expressed genes in the VAT

pathway name	set size	candidates contained	p-value	q-value
Valine, leucine and isoleucine degradation - Homo sapiens (human)	44	16 (36.4%)	7.58e-20	6.67e-18
Citrate cycle (TCA cycle) - Homo sapiens (human)	30	10 (33.3%)	2.26e-12	9.96e-11
Pyruvate metabolism - Homo sapiens (human)	41	10 (24.4%)	7.48e-11	2.2e-09
Propanoate metabolism - Homo sapiens (human)	32	9 (28.1%)	1.69e-10	3.72e-09
Glyoxylate and dicarboxylate metabolism - Homo sapiens (human)	24	7 (29.2%)	1.5e-08	2.63e-07
Butanoate metabolism - Homo sapiens (human)	29	7 (24.1%)	6.39e-08	9.38e-07
Fatty acid metabolism - Homo sapiens (human)	44	8 (18.2%)	7.64e-08	9.6e-07
Insulin signaling pathway - Homo sapiens (human)	139	11 (8.0%)	1.61e-06	1.77e-05
Peroxisome - Homo sapiens (human)	81	8 (10.0%)	8.45e-06	8.26e-05
Fatty acid elongation - Homo sapiens (human)	23	5 (21.7%)	9.4e-06	8.27e-05
Tryptophan metabolism - Homo sapiens (human)	40	6 (15.0%)	1.12e-05	8.98e-05
Glycolysis / Gluconeogenesis - Homo sapiens (human)	65	7 (10.8%)	1.94e-05	0.000142
Lysine degradation - Homo sapiens (human)	49	6 (12.5%)	3.3e-05	0.000223
Alanine, aspartate and glutamate metabolism - Homo sapiens (human)	32	5 (15.6%)	5.12e-05	0.000322
beta-Alanine metabolism - Homo sapiens (human)	29	4 (13.8%)	0.000495	0.00291
Arginine and proline metabolism - Homo sapiens (human)	57	5 (8.8%)	0.000822	0.00452
Biosynthesis of unsaturated fatty acids - Homo sapiens (human)	21	3 (14.3%)	0.00238	0.0118
Fatty acid biosynthesis - Homo sapiens (human)	6	2 (33.3%)	0.00241	0.0118
Type II diabetes mellitus - Homo sapiens (human)	48	4 (8.3%)	0.00336	0.0156
Synthesis and degradation of ketone bodies - Homo sapiens (human)	9	2 (22.2%)	0.00564	0.0248
Galactose metabolism - Homo sapiens (human)	29	3 (10.3%)	0.00605	0.0254

Significantly differentially expressed genes in the VAT were mapped onto the KEGG pathway for over- representation analysis using the software tool made available by ConsensusPathDB. 'Pathway names' contains the names of the significant pathways, 'set size' is the number of genes in the pathway, 'candidates contained' is the number of genes in the input that are members of the pathway. The p- value is calculated according to the hypergeometric test based on the number of genes present in both the predefined set and list of significant genes from VAT provided as input. The p-values are corrected for multiple testing using false discovery rate and are shown as q-values above. The results provided in the table above are for a q-value cut-off of < 0.05.

ESM Table 4: KEGG Pathway over-representation analysis among significantly differentially expressed genes in the SAT

pathway name	set size	candidates contained	p-value	q-value
Shigellosis - Homo sapiens (human)	61	6 (9.8%)	7.48e-06	0.00116
Salmonella infection - Homo sapiens (human)	88	6 (7.0%)	5.43e-05	0.00421
Fc gamma R-mediated phagocytosis - Homo sapiens (human)	94	6 (6.4%)	8.94e-05	0.00462
Leishmaniasis - Homo sapiens (human)	76	5 (6.9%)	0.00024	0.0064
Regulation of actin cytoskeleton - Homo sapiens (human)	215	8 (3.8%)	0.000249	0.0064
Pyruvate metabolism - Homo sapiens (human)	41	4 (9.8%)	0.000282	0.0064
Bacterial invasion of epithelial cells - Homo sapiens (human)	77	5 (6.5%)	0.000329	0.0064
Branched-chain amino acid catabolism	18	3 (16.7%)	0.000345	0.0064
Valine, leucine and isoleucine degradation - Homo sapiens (human)	44	4 (9.1%)	0.000372	0.0064
Sema4D induced cell migration and growth-cone collapse	26	3 (11.5%)	0.00105	0.0163
Platelet activation, signaling and aggregation	214	7 (3.3%)	0.00132	0.0186
Cross-presentation of particulate exogenous antigens (phagosomes)	8	2 (25.0%)	0.00164	0.0201
Sema4D in semaphorin signaling	31	3 (9.7%)	0.00177	0.0201
Semaphorin interactions	68	4 (5.9%)	0.00194	0.0201
GPVI-mediated activation cascade	32	3 (9.4%)	0.00194	0.0201
Hyaluronan uptake and degradation	9	2 (22.2%)	0.0021	0.0203
Leukocyte transendothelial migration - Homo sapiens (human)	118	5 (4.2%)	0.00227	0.0207
Adherens junction - Homo sapiens (human)	73	4 (5.5%)	0.00251	0.0213
Hyaluronan metabolism	10	2 (20.0%)	0.00261	0.0213
The NLRP3 inflammasome	11	2 (18.2%)	0.00318	0.0246
Hemostasis	472	10 (2.1%)	0.00341	0.0251
Osteoclast differentiation - Homo sapiens (human)	135	5 (3.8%)	0.00381	0.0266
Platelet degranulation	86	4 (4.8%)	0.00417	0.0266
Insulin signaling pathway - Homo sapiens (human)	139	5 (3.6%)	0.00445	0.0266
Natural killer cell mediated cytotoxicity - Homo sapiens (human)	140	5 (3.6%)	0.00445	0.0266
Signal regulatory protein (SIRP) family interactions	14	2 (15.4%)	0.00446	0.0266
Response to elevated platelet cytosolic Ca2+	91	4 (4.5%)	0.00513	0.0294
Type II diabetes mellitus - Homo sapiens (human)	48	3 (6.2%)	0.00619	0.0343
Inflammasomes	16	2 (12.5%)	0.00675	0.0355
Phagosome - Homo sapiens (human)	157	5 (3.3%)	0.00687	0.0355
Platelet sensitization by LDL	18	2 (11.8%)	0.00762	0.0379
Regulation of actin dynamics for phagocytic cup formation	103	4 (4.0%)	0.00799	0.0379
Metabolism	1374	19 (1.4%)	0.00807	0.0379
Steroid biosynthesis - Homo sapiens (human)	18	2 (11.1%)	0.00853	0.0389
Pathogenic Escherichia coli infection - Homo sapiens (human)	55	3 (5.5%)	0.00903	0.04
Growth hormone receptor signaling	19	2 (10.5%)	0.00948	0.0408

Significantly differentially expressed genes in the SAT were mapped onto the KEGG pathway for over- representation analysis using the software tool made available by ConsensusPathDB. 'Pathway names' contains the names of the significant pathways, 'set size' is the number of genes in the pathway, 'candidates contained' is the number of genes in the input that are members of the pathway. The p-value is calculated according to the hypergeometric test based on the number of genes present in both the predefined set and list of significant genes from SAT provided as input. The p-values are corrected for multiple testing using false discovery rate and are shown as q-values above. The results provided in the table above are for a q-value cut-off of < 0.05.

ESM Table 5: Top 15 Enriched Network-based Sets (NESTs) for an input of top hits from the visceral adipose tissue differentially expressed between diabetic and healthy subjects.

set centers	radius	set size	candidates contained	p-value	q-value
HADHA	1	343	25 (7.3%)	1.54e-15	3.24e-12
2-methyl-3-hydroxybutyryl-CoA dehydrogenase	1	299	21 (7.0%)	6.88e-13	7.26e-10
EHHADH	1	69	12 (17.4%)	1.75e-12	1.23e-09
mitochondrial 3-ketoacyl-CoA thiolase monomer	1	80	12 (15.0%)	1.1e-11	5.52e-09
Dihydrolipoamide dehydrogenase, mitochondrial	1	276	19 (6.9%)	1.31e-11	5.52e-09
3,2-trans-enoyl-CoA isomerase, mitochondrial precursor	1	251	18 (7.2%)	2.36e-11	8.3e-09
SDHA	1	291	19 (6.6%)	3.1e-11	9.34e-09
ATP synthase beta chain	1	416	22 (5.3%)	5.01e-11	1.32e-08
Acyl-CoA dehydrogenase, long-chain specific, mitochondrial precursor	1	28	8 (28.6%)	1.36e-10	3.19e-08
2,4-dienoyl-CoA reductase-related protein	1	20	7 (35.0%)	4e-10	8.07e-08
ssbp_human	1	299	18 (6.0%)	4.21e-10	8.07e-08
rm15_human	1	267	17 (6.4%)	5.59e-10	9.6e-08
rm49_human	1	268	17 (6.4%)	5.92e-10	9.6e-08
ALDH1B1 : aldehyde dehydrogenase 1 family, member B1	1	273	17 (6.3%)	7.44e-10	1.12e-07
Acyl-CoA dehydrogenase, short-chain specific, mitochondrial precursor	1	13	6 (46.2%)	1.02e-09	1.44e-07
PDK3	1	245	16 (6.6%)	1.27e-09	1.68e-07

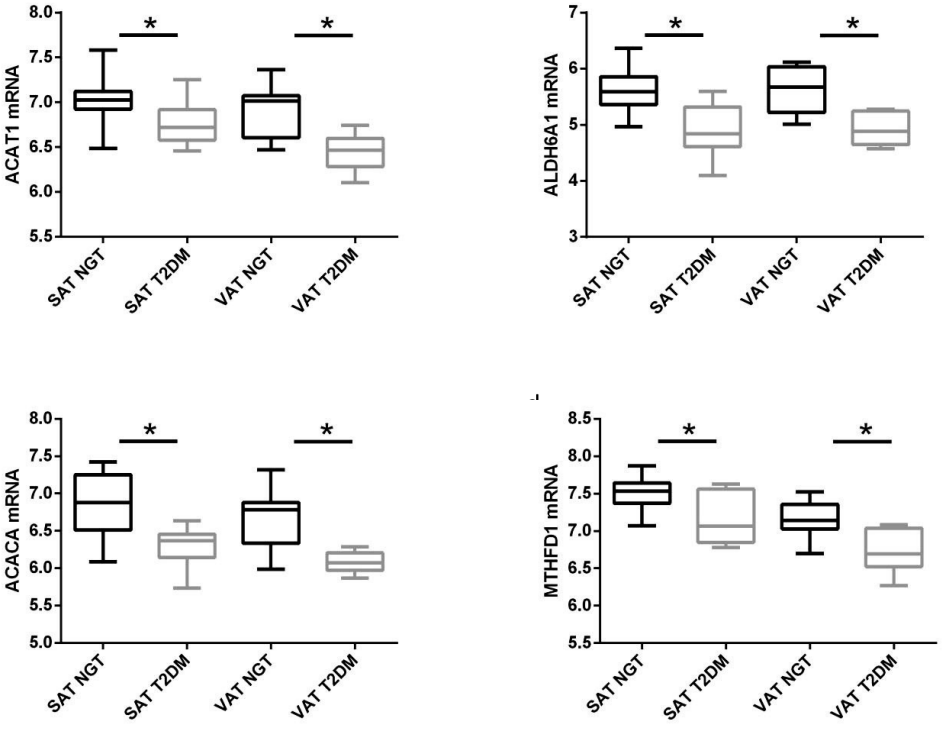

ESM Fig. 1a-d: No difference in adipose tissue expression of a) ACAT1, b) ACACA, c) ALDH6A1 or d) MTHFD1 between T2DM subjects that use metformin and those that do not use metformin. Boxplots of normalized gene expression profiles (log2-scale) are shown. (SAT = subcutaneous adipose tissue, VAT = visceral adipose tissue)

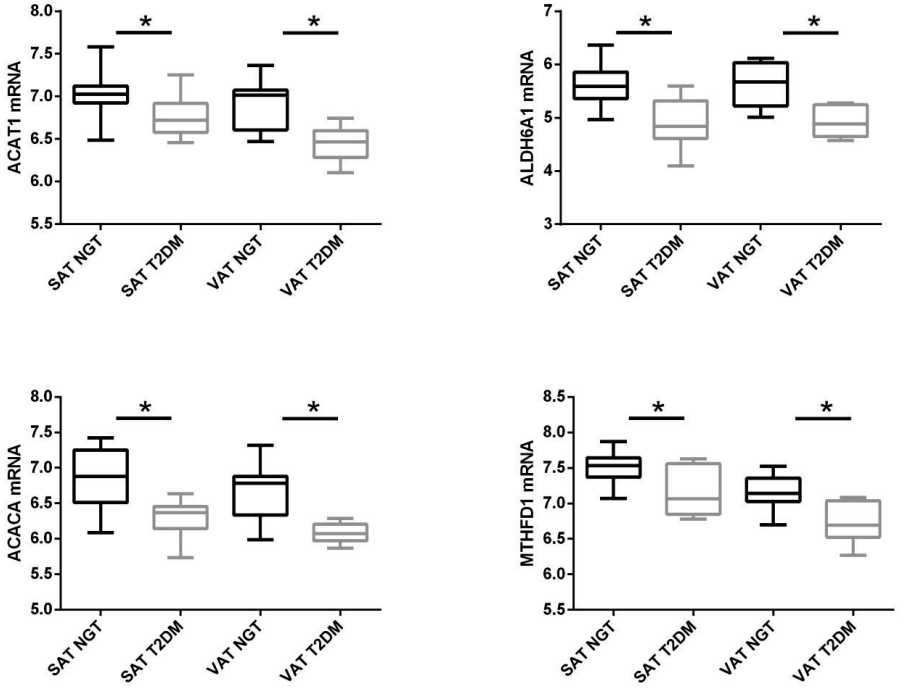

ESM Fig. 2a-d: The comparison of adipose tissue gene expression of ACAT1, ACACA, ALDH6A1 and MTHFD1 between NGT and T2DM subjects when all metformin users are excluded. The acetyl coA genes are lower in the T2DM subjects. Boxplots of normalized gene expression profiles (log2-scale) are shown. (SAT = subcutaneous adipose tissue, VAT = visceral adipose tissue)

References (Supplemental section)

1 Wu TD, Nacu S: **Fast and SNP-tolerant detection of complex variants and splicing in short reads**. *Bioinformatics* 2010, **26**(7):873-881.

2. Li H, Handsaker B, Wysoker A, Fennell T, Ruan J, Homer N, Marth G, Abecasis G, Durbin R, Genome Project Data Processing S: **The Sequence Alignment/Map format and SAMtools**. *Bioinformatics* 2009, **25**(16):2078-2079.

3. Dale RK, Pedersen BS, Quinlan AR: **Pybedtools: a flexible Python library for manipulating genomic datasets and annotations**. *Bioinformatics* 2011, **27**(24):3423-3424.

4. Robinson MD, McCarthy DJ, Smyth GK: **edgeR: a Bioconductor package for differential expression analysis of digital gene expression data**. *Bioinformatics* 2010, **26**(1):139-140.

5. Law CW, Chen Y, Shi W, Smyth GK: **Voom: precision weights unlock linear model analysis tools for RNA-seq read counts.** *Genome Biol* 2014, **15**:R29.

6. Wolstencroft K, Haines R, Fellows D, Williams A, Withers D, Owen S, Soiland-Reyes S, Dunlop I, Nenadic A, Fisher P *et al*: **The Taverna workflow suite: designing and executing workflows of Web Services on the desktop, web or in the cloud**. *Nucleic acids research* 2013, **41**(Web Server issue):W557-561.

7. Dharuri H, Henneman P, Demirkan A, van Klinken JB, Mook-Kanamori DO, Wang-Sattler R, Gieger C, Adamski J, Hettne K, Roos M *et al*: **Automated workflow-based exploitation of pathway databases provides new insights into genetic associations of metabolite profiles**. *BMC genomics* 2013, **14**(1):865.

8. Kanehisa M, Goto S, Furumichi M, Tanabe M, Hirakawa M: **KEGG for representation and analysis of molecular networks involving diseases and drugs**. *Nucleic acids research* 2010, **38**(Database issue):D355-360.